

UC Berkeley

UC Berkeley Previously Published Works

Title

Hydrogenation of butanal over silica-supported Shvo's catalyst and its use for the gas-phase conversion of propene to butanol via tandem hydroformylation and hydrogenation

Permalink

<https://escholarship.org/uc/item/35r940xx>

Authors

Hanna, David G
Shylesh, Sankaranarayanapillai
Parada, Pedro A
[et al.](#)

Publication Date

2014-03-01

DOI

10.1016/j.jcat.2013.11.012

Peer reviewed



Hydrogenation of butanal over silica-supported Shvo's catalyst and its use for the gas-phase conversion of propene to butanol via tandem hydroformylation and hydrogenation



David G. Hanna, Sankaranarayananpillai Shylesh, Pedro A. Parada, Alexis T. Bell*

Department of Chemical and Biomolecular Engineering, University of California, Berkeley, CA 94720, USA

ARTICLE INFO

Article history:

Received 27 August 2013

Revised 1 November 2013

Accepted 12 November 2013

Available online 15 December 2013

Keywords:

Butanal
Hydrogenation
Butanol
Shvo
Kinetics

ABSTRACT

The objective of the present study was to develop a heterogeneous catalyst for the hydrogenation of butanal that could function in the presence of CO and propene and, hence, could be used in a tandem reactor to enable the gas-phase conversion of propene and synthesis gas to butanol. To this end, we investigated the activity of silica-supported Shvo's catalyst (Shvo/SiO₂) for the gas-phase hydrogenation of butanal. Experiments were performed to determine the kinetics of *n*- and iso-butanol hydrogenation. The apparent activation energies and the apparent partial pressure dependencies of *n*- and iso-butanol, H₂, and CO on the rates of *n*- and iso-butanol formation were determined. A mechanism for butanal hydrogenation was proposed to rationalize the observed kinetics and some of the reaction intermediates were observed by in situ infrared and ³¹P MAS NMR spectroscopy. It was found that Shvo/SiO₂ was inhibited by SX (SX = sulfoxanthphos) and CO, and is inactive for alkene hydrogenation. The tandem catalytic conversion of propene and synthesis gas to butanol was then carried out using a SX-Rh supported ionic liquid phase (SILP) catalyst to promote the hydroformylation of propene to butanal and Shvo/SiO₂ to promote the hydrogenation of butanal to butanol. The rate expressions describing the kinetics of each of the catalysts were then used to predict operating conditions required to achieve high conversion of propene to butanol. Under the most favorable conditions examined (H₂/CO = 10), an overall yield of 13% to butanol was achieved with 15% propene conversion and 90% aldehyde conversion at a temperature of 413 K.

© 2013 Elsevier Inc. All rights reserved.

1. Introduction

Roughly 2×10^6 tons of butanol are produced annually [1] for use as a plasticizer, an industrial solvent, and an intermediate in the production of butyl acetate, a key ingredient in lacquers and varnishes [2]. The demand for butanol is expected to increase in the future as a consequence of recent studies showing that butanol is a viable alternative to ethanol as an additive to gasoline [3,4].

While many processes exist for the production of butanol, such as the aldol condensation of ethanal [5], oxidation of butane [6], or the enzymatic fermentation of sugars [3,7], the overwhelming majority of butanol is produced in a three-step process involving the homogeneously catalyzed hydroformylation of propene, separation of the resulting butanal, and subsequent hydrogenation of butanal. Separation of butanal is necessary because aldehyde hydrogenation catalysts such as supported Pt and Pt–Sn [8], Rh–Sn [9], and Ni [10] are poisoned by CO, as well as being active for alkene hydrogenation. Therefore, it would be highly desirable to develop a catalyst system for the tandem, gas-phase conversion

of propene and synthesis gas to butanol. Achievement of this goal requires identification of a heterogeneous hydroformylation catalyst and a heterogeneous aldehyde hydrogenation catalyst that functions in the presence of CO and is inactive for alkene hydrogenation.

Recent studies have shown that the gas-phase hydroformylation of propene can be carried out on a heterogeneous catalyst prepared by impregnating a Rh–phosphine complex dissolved in ionic liquid onto a silica support [11,12]. Such catalysts, referred to as supported ionic liquid phase (SILP) catalysts, are stable and active under continuous gas-phase reaction conditions. We have recently shown that the exceptional stability of these catalysts is due to the interaction of the Rh–phosphine complex with silanol groups present on the support surface and have discussed the mechanism and kinetics propene hydroformylation over this catalyst [13,14].

Several attempts to perform the tandem conversion of C_n alkenes and synthesis gas to the C_{n+1} alcohol in a single reactor system have been reported. Drent and coworkers have shown that chloride anion promoted palladium–phosphine complexes could be used to convert propene to *n*- and iso-butanol with 85% selectivity [15]. High turnovers (1000 h^{−1}) and selectivity (99%) were also observed in the conversion of C8–C10 internal alkenes into their

* Corresponding author. Fax: +1 510 642 4778.

E-mail address: bell@cchem.berkeley.edu (A.T. Bell).

corresponding alcohols [15]. A halogen-free system studied by Zakzeski et al. demonstrated that the conversion of hexene to heptanol could be achieved utilizing $\text{HRh}(\text{PPh}_3)_2(\text{CO})$ as the hydroformylation catalyst and $\text{H}_2\text{Ru}(\text{PPh}_3)_3\text{CO}$ as the hydrogenation catalyst [16]. It was noted, though, that the hydrogenation of the aldehyde would only occur after the CO was consumed or removed from the reactor because the Ru complex was inhibited by CO [16]. More recently, Nozaki and coworkers have demonstrated that it is possible to carry out the hydroformylation of propene to butanol and the subsequent hydrogenation of butanal to butanol in a solution containing a Rh complex, Shvo's catalyst, and bidentate phosphine ligand, sulfoxantphos (SX) [17]. Using this approach, butanol yields of up to 85% were obtained [17]. The authors suggest that the presence of excess SX influences the activity and/or the chemoselectivity of Shvo's catalyst to preferentially hydrogenate aldehydes [17]. These findings motivated us to explore the possibility of supporting Shvo's catalyst on silica in order to produce a heterogeneous catalyst that could be used in a tandem, gas-phase hydroformylation–hydrogenation process. In this work, we report the successful preparation of a silica-supported Shvo's catalyst, present the kinetics of *n*- and iso-butanol hydrogenation, and discuss the effects of CO on the hydrogenation activity. The activity of SX-modified silica-supported Shvo's catalyst was also investigated to test whether the presence of a phosphine ligand enhances the activity and/or improves the CO tolerance. We also show that silica-supported Shvo's catalyst can be used in tandem with a SX-Rh SILP catalyst to carry out the direct synthesis of butanol from propene and synthesis gas.

2. Material and methods

2.1. Catalyst synthesis

Approximately, 0.06 g of 1-hydroxytetraphenylcyclopentadienyl (tetraphenyl-2,4-cyclopentadien-1-one)- μ -hydrotetracarbonyldiruthenium(II), Shvo's catalyst, (Strem, 98%) was dissolved in 10 mL of anhydrous methanol (Aldrich, 99.8%). After 10 min of stirring, 1 g of silica (Silicycle, $500 \text{ m}^2 \text{ g}^{-1}$, average pore diameter 60 Å) stored under vacuum at 353 K was added to solution and stirred for an additional 1 h. Methanol was then slowly removed under vacuum in a rotary evaporator. The resulting catalyst is a yellowish-orange colored powder containing 0.4 wt.% Ru. SX-Shvo/SiO₂ was prepared in a similar manner except that in this case, sulfoxantphos (SX) [18] was added to the solution prior to the addition of SiO₂. Approximately 434 mg of SX was used to achieve a molar ratio of SX/Ru = 5.

2.2. Measurements of catalyst activity

Measurements of reaction rates were performed in a 6.35 mm OD quartz tube containing an expanded section (~ 12.7 mm OD, ~ 20 mm length). A plug of quartz wool was placed below the catalyst bed to hold the powder in place. The reactor was heated by a ceramic furnace with external temperature control and the catalyst bed temperature was measured with a K-type thermocouple sheathed in a quartz capillary placed in direct contact with the catalyst bed.

Prior to reaction, 0.3 g of catalyst was heated to the reaction temperature at a rate of 2 K min^{-1} in pure He (Praxair, 99.999%) flowing at $20 \text{ cm}^3 \text{ min}^{-1}$ at STP. The feed to the reactor consisted of *n*-butanal (Aldrich, 98%), iso-butanal (Aldrich, 99%), H₂ (Praxair, 99.999%), and He (Praxair, 99.999%). CO (Praxair, 99.99%) was passed through a trap packed with 3.2 mm pellets of 3 Å molecular sieve in order to remove iron pentacarbonyl formed within the cylinder [19] and was then co-fed with the other reactants. An

equimolar mixture of *n*- and iso-butanol was placed in a 5-mL syringe connected to a syringe pump (Cole-Palmer, 74900 series). The liquid mixture was injected into a heated port subjected to continuous flow of He. A molar ratio of butanal to H₂ of 1:1 was used unless specified otherwise. Experiments were carried out at a total gas pressure of 1 atm. The total gas flow rate was typically $100 \text{ cm}^3 \text{ min}^{-1}$ at STP. Using these conditions, the conversion of aldehyde was always less than 10%. Reaction products were analyzed using an Agilent 6890N gas chromatograph containing a bonded and crosslinked (5%-Phenyl)-methylpolysiloxane capillary column (Agilent, HP-1) connected to a flame ionization detector (FID).

The continuous gas-phase hydrogenation of butene was also examined in order to determine the activity of Shvo/SiO₂ for alkene hydrogenation. Prior to reaction, 0.3 g of Shvo/SiO₂ catalyst was heated to 363 K at a rate of 2 K min^{-1} in pure He (Praxair, 99.999%) flowing at $20 \text{ cm}^3 \text{ min}^{-1}$ at STP. The feed to the reactor was then switched to one containing 1-butene (Praxair, 99.9%), H₂ (Praxair, 99.999%), and He (Praxair, 99.999%). A 1:1 stoichiometric ratio of 1-butene to H₂ was introduced to reactor at 1 atm. The partial pressure of 1-butene and He was 0.05 atm and 0.9 atm, respectively. The total gas flow rate was $100 \text{ cm}^3 \text{ min}^{-1}$ at STP. Reaction products were analyzed using a gas chromatograph–mass spectrometer (Varian, Model 320) equipped with a 14-port sampling valve and three sample loops. One sample loop was injected into an Alumina PLOT column for the FID and mass spectrometer, and the other sample loop was injected into a Hayesep and Mol Sieve packed columns.

2.3. Gas-phase hydroformylation and hydrogenation of propene to butanol

Tandem hydroformylation and hydrogenation experiments were conducted using a procedure similar to that described in Section 2.2. A bi-layered catalyst bed consisting of Rh-SILP and Shvo/SiO₂ catalysts was utilized. The SILP catalyst was prepared as described in Refs. [13,14]. Shvo/SiO₂ and Rh-SILP were loaded sequentially into the reactor (so that SILP catalyst was at the top) along with an intermediary layer of quartz wool to minimize the mixing of the two catalysts. Prior to reaction, the reactor was heated to 413 K at a rate of 2 K min^{-1} in pure He (Praxair, 99.999%) flowing at $20 \text{ cm}^3 \text{ min}^{-1}$ at STP. Experiments were carried out at total gas pressures varying from 1 to 3 atm and the feed to the reactor consisted of propene (Praxair, 99.9%), CO (Praxair, 99.99%), H₂ (Praxair, 99.999%), and He (Praxair, 99.999%). The total gas flow rate varied from 20 to $60 \text{ cm}^3 \text{ min}^{-1}$ at STP in order to maintain a constant residence time. The reaction products were analyzed by a Agilent 6890N gas chromatograph equipped with a HP-1 column connected to a FID.

2.4. In situ infrared spectroscopy

Infrared spectra were acquired using a Thermo Scientific Nicolet 6700 FTIR spectrometer equipped with a liquid nitrogen cooled MCT detector. Each spectrum was obtained by averaging 32 scans taken with 1 cm^{-1} resolution. 0.015 g of Shvo/SiO₂ or SX-Shvo/SiO₂ was pressed into a 20 mm-diameter pellet ($< 1 \text{ mm}$ thick) and placed into a custom-built transmission cell equipped with CaF₂ windows, a K-type thermocouple for temperature control, and resistive cartridge heaters similar to that described in Ref. [20]. All scans were acquired at 363 K and 1 atm. All absorption spectra were taken relative to the empty transmission cell. The spectrum of the catalyst under He flow was subtracted from all the results reported.

2.5. Solid-state ^{31}P MAS NMR

Solid-state ^{31}P MAS NMR experiments were performed on a Bruker Avance I-500 MHz spectrometer. Data were obtained by measuring the samples using a frequency of 202.5 MHz, 90° pulse in 4.2 μs , and a delay of 60 s.

3. Results and discussion

3.1. Catalyst stability and kinetics of butanal hydrogenation

To investigate the stability of SX-Shvo/SiO₂ and Shvo/SiO₂ with time-on-stream, experiments were conducted using an equimolar gas mixture of H₂ and *n*-butanal. As shown in Fig. 1a, both catalysts were stable, although the activity of SX-Shvo/SiO₂ was nearly 50% lower than that of Shvo/SiO₂. Fig. 1b shows that the addition of CO to the feed after 2 h of time on stream decreased the butanal hydrogenation activity of both catalysts quite substantially. The turnover frequency of SX-Shvo/SiO₂ and Shvo/SiO₂ dropped from roughly 8 h⁻¹ to 3 h⁻¹ and 4 h⁻¹ to 2 h⁻¹, respectively.

Table 1 lists the apparent activation barriers for Shvo/SiO₂ and SX-Shvo/SiO₂ catalysts measured in the temperature range 343–373 K. The apparent activation energy for aldehyde hydrogenation to *n*-butanol and iso-butanol with Shvo/SiO₂ are 50 kJ mol⁻¹ and 49 kJ mol⁻¹, respectively. Similar activation energies were also measured for SX-Shvo/SiO₂, 46 kJ mol⁻¹ and 51 kJ mol⁻¹ for *n*- and iso-butanol, respectively.

To determine the apparent reaction orders of *n*- and iso-butanol, H₂, and CO on the rate of butanol formation, the partial pressures of two components were fixed while the partial pressures of the third reactant and He were varied. The total gas flow rate was kept at 100 cm³ min⁻¹ at STP in order to maintain a constant residence time. Table 2 shows the effects of varying the partial pressures of H₂, *n*- and iso-butanol, and CO on the rate of formation of *n*- and iso-butanol over Shvo/SiO₂ and SX-Shvo/SiO₂. The partial pressure dependencies and catalytic rates are nearly equal for *n*- and iso-butanol formation. The orders with respect to H₂, *n*-butanol, and CO on the rate of formation of *n*-butanol are 0.26, 1.0, and -0.59, respectively. Similarly, the orders with respect to H₂, iso-butanol, and CO on the rate of formation of iso-butanol are 0.29, 1.1, and -0.58, respectively. The apparent reaction orders of H₂ and CO increased in the presence of SX. The partial pressure dependencies of H₂, *n*-butanol, and CO on the rate of formation of *n*-butanol are 0.42, 0.98, and -0.29, respectively, while the

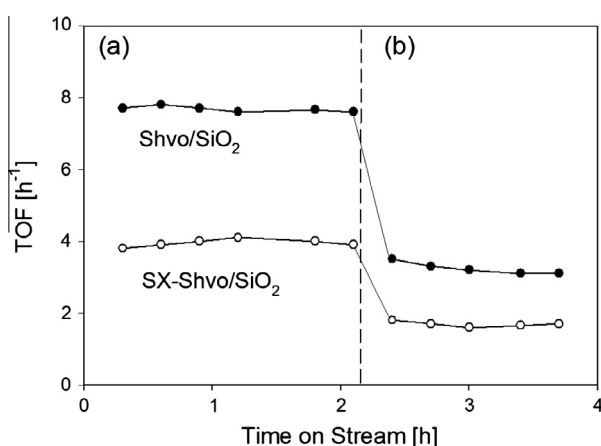


Fig. 1. (a and b) Time on stream study with (●) Shvo/SiO₂ and (○) SX-Shvo/SiO₂ catalysts, $T = 363\text{ K}$, $P_{\text{Total}} = 1\text{ atm}$, catalyst mass = 0.3 g, total gas flow rate at STP = 100 cm³ min⁻¹. (a) $P_{\text{H}_2} = P_{\text{butanal}} = 0.05\text{ atm}$, balance He. (b) $P_{\text{CO}} = P_{\text{H}_2} = P_{\text{butanal}} = 0.05\text{ atm}$, balance He.

Table 1

Apparent activation energies (kJ mol⁻¹) for the formation of *n*- and iso-butanol using Shvo/SiO₂ or SX-Shvo/SiO₂. $T = 343\text{--}373\text{ K}$, $P_{\text{Total}} = 1\text{ atm}$, $P_{\text{H}_2} = P_{\text{butanal}} = 0.05\text{ atm}$, balance He. Total gas flow rate = 100 cm³ min⁻¹, catalyst mass = 0.3 g.

Catalyst	Apparent activation energy (kJ mol ⁻¹)	
	<i>n</i> -Butanol	iso-Butanol
Shvo/SiO ₂	49	50
SX-Shvo/SiO ₂	46	51

partial pressure dependencies of H₂, iso-butanol, and CO on the rate of iso-butanol formation are 0.45, 0.95, and -0.31, respectively over SX-Shvo/SiO₂ catalysts.

3.2. Proposed mechanism of butanal hydrogenation

The kinetics of butanal formation can be interpreted using the mechanism proposed by Shvo and coworkers [21,22] shown in Scheme 1. Shvo's catalyst operates through a concerted, outer-sphere mechanism in which the aldehyde is reduced in one elementary step despite not being bound directly to the metal [23]. The reaction sequence begins with the dissociation of the dimeric Ru complex (Shvo's catalyst, species A) into the constitutive monomers species B and C (Reaction 1). Butanal coordinates to the outer sphere of the complex by aligning the polarity of the acetyl group (partially positively charged carbon and partially negatively charged oxygen) with the hydridic (H–Ru) and acidic hydrogen (H–O) present on species C. The bound aldehyde is then reduced to alcohol, which converts species C into species B (Reaction 3). The catalytic cycle is closed by reaction of H₂ with species B to yield species C (Reaction 2). Species B has a vacant coordination site and therefore can react with either ligand, CO or SX, via Reactions 4 or 5 respectively to fulfill the vacancy. Species D and E are both saturated species which must dissociate a ligand to be catalytically active.

Evidence for the existence of several of the intermediates shown in Scheme 1 was provided by in situ infrared spectroscopy. Fig. 2 shows IR spectra of the pristine Shvo's complex and Shvo/SiO₂ under exposure of He at 298 K, He at 363 K, an equimolar mixture of H₂ and He at 363 K, and an equimolar mixture of H₂, CO, and He at 363 K. The peak in spectra A and B at 1713 cm⁻¹ is ascribed to the bridging O–H–O bond present in the Ru dimer [21,24], while the broad peak at 1875 cm⁻¹ in spectrum B is from the SiO₂ support as shown by Fig. S1 in the Supporting information. Spectrum C shows that as the reaction temperature was increased to 363 K, the band at 1713 cm⁻¹ disappeared while bands at 1965, 2005, and 2030 cm⁻¹ became better resolved. The disappearance of the 1713 cm⁻¹ band with increased temperature indicates that the Ru dimer complex has dissociated into its constitutive monomers. The bands appearing at 1965, 2005, and 2030 cm⁻¹ are characteristic of carbonyl ligands bound to species B and species C [25,26] and are sharper in spectrum B than in spectrum A due to the removal of physisorbed water on the SiO₂ surface at elevated temperature. The appearance of a broad band at 1630 cm⁻¹ is attributed to the oxo functionality present on the cyclopentadienyl ligand of species B which is another indication that the Ru dimer has dissociated into Ru monomer units. Once the catalyst is treated with H₂ (spectrum D), a negative band appears at 1630 cm⁻¹ upon subtraction from spectrum B signifying the conversion of species B into species C via Reaction 2. Exposure of the catalyst to CO, as shown in spectrum E, causes two new bands to appear at 2100 and 2050 cm⁻¹, while the band at 1965 cm⁻¹ becomes negative upon subtraction from spectrum B. The new bands in the carbonyl stretching region are attributed to the transformation of species B into a tricarbonyl Ru complex species E.

Table 2

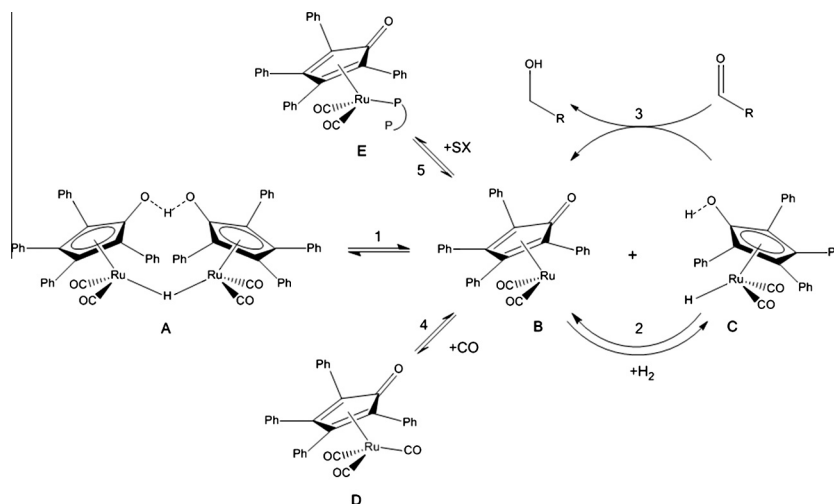
Apparent reaction orders of *n*-butanol and iso-butanol synthesis using Shvo/SiO₂ and SX-Shvo/SiO₂ catalysts. *T* = 363 K, *P*_{Total} = 1 atm, catalyst mass = 0.3 g, total gas flow rate = 100 cm³ min⁻¹.

Reaction product	Catalyst	Apparent reaction order		
		H ₂ ^a	Butanal ^b	CO ^c
<i>n</i> -Butanol	Shvo/SiO ₂	0.26	1.0	-0.59
	SX-Shvo/SiO ₂	0.42	0.98	-0.29
iso-Butanol	Shvo/SiO ₂	0.29	1.1	-0.58
	SX-Shvo/SiO ₂	0.45	0.95	-0.31

^a *P*_{H₂} = [0.05–0.15 atm], *P*_{*n*-butanal} = *P*_{iso-butanal} = 0.025 atm, balance He.

^b *P*_{*n*-butanal} = *P*_{iso-butanal} = [0.025–0.075 atm], *P*_{H₂} = 0.05 atm, balance He.

^c *P*_{CO} = [0.05–0.15 atm], *P*_{H₂} 0.05 atm, *P*_{*n*-butanal} = *P*_{iso-butanal} = 0.025 atm, balance He.



Scheme 1. Proposed mechanism for aldehyde hydrogenation using Shvo/SiO₂ catalyst.

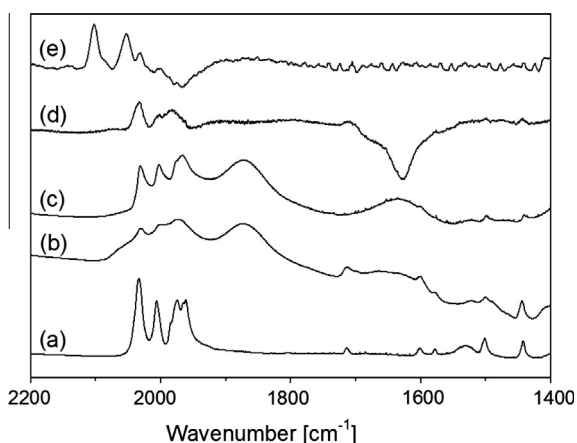


Fig. 2. In situ infrared spectra of (a) Shvo's complex in He at 298 K and Shvo/SiO₂ catalyst under, (b) He at 298 K, (c) He at 363 K, (d) H₂ at 363 K, and (e) H₂/CO = 1 at 363 K.

The spectra for SX-Shvo/SiO₂ exhibit similar bands to those observed for Shvo/SiO₂. The most notable difference between the catalysts is that the carbonyl stretching region is red-shifted by 5–10 cm⁻¹ in the presence of SX because phosphines are better sigma donors than carbonyl ligands [27]. The higher electron density on Ru enables greater pi-backbonding to the carbonyl groups, thereby reducing the frequency of the carbonyl stretching frequency. A comparison of the spectra for Shvo/SiO₂ and SX-Shvo/SiO₂ is provided in the Supporting information.

Further evidence for the coordination of SX to Shvo's catalysts under reaction conditions was obtained from ³¹P NMR spectroscopy. Fig. 3 shows the results of solid-state ³¹P MAS NMR measurements of spent SX-Shvo/SiO₂ which exhibits the same spectral features of the fresh SX-Shvo/SiO₂. The broad peak observed at -13 ppm can be ascribed to the free SX adsorbed on the silica surface [13], while the broad peak centered at 34 ppm is due to the phosphine bonded to Ru as shown in species E [17]. Although many of species shown in Scheme 1 could undergo ligand exchange with SX, Reaction 5 is the most facile because of the vacant coordination site on species B. Previous reports that have shown by solution ³¹P NMR that singly coordinated phosphorus to Ru

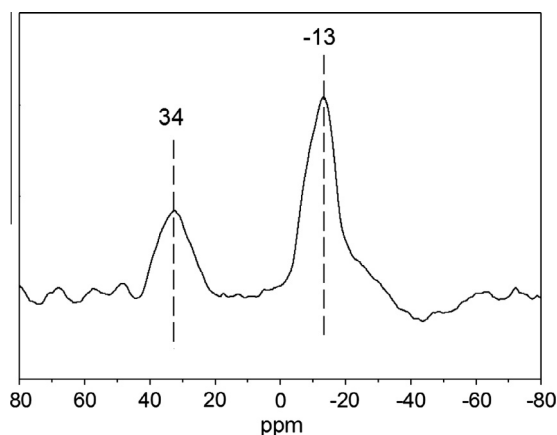


Fig. 3. Solid-state ³¹P MAS NMR spectra of spent SX-Shvo/SiO₂ catalyst.

(species **E** of Scheme 1) results from the reaction of species **B** with SX [17]. However, the possibility that both phosphorus atoms of SX are coordinated to Ru cannot be ruled out on the basis of the present data. While there have reports indicating that Shvo's catalyst modified with PPh₃ can complete the catalytic cycle, this occurs at much slower rates than with the unmodified catalysts [28]; thus, all of the catalytic activity is attributed to unmodified species **C**. The data and the literature, therefore, indicate that SX-Shvo/SiO₂ is less active than Shvo/SiO₂ because coordination of SX reduces the concentration of species **C** available for the catalytic cycle.

3.3. Kinetics of butanal hydrogenation

If it is assumed that at reaction temperature, species **A** dissociates completely to species **B** and **C**, that Reactions 2, 4, and 5 are quasi-equilibrated, and that Reaction 3 is the irreversible, rate-limiting step, then the rate of butanol formation is given by the following relation:

$$r_{\text{butanol}} = \frac{K_2 k_3 P_{\text{butanal}} P_{\text{H}_2} [\text{Ru}]}{1 + K_2 P_{\text{H}_2} + K_4 P_{\text{CO}} + K_5 [\text{SX}]} \quad (1)$$

where k_3 is the rate coefficient for Reaction 3, K_i is the equilibrium constant for Reaction i , P_j is the partial pressure of species j , and $[\text{Ru}]$ is the total surface concentration of Ru. The derivation of Eq. (1) is provided in the Supporting information.

Eq. (1) is consistent with the experimentally observed partial pressure dependencies and those found in literature. Casey and coworkers have reported that the order with respect to benzaldehyde and H₂ in a homogenous solution of Shvo's Catalyst to be 1 and 0, respectively [28]. The rate of butanal synthesis is first order in butanal due to the P_{butanal} term in the numerator of Eq. (1). The 0–1 order in the partial pressure of H₂ depends on the magnitude of the $K_2 P_{\text{H}_2}$ in the denominator of Eq. (1). As the value of $K_2 P_{\text{H}_2}$ increases, the order with respect to H₂ tends toward zero. Thus, the value for $K_2 P_{\text{H}_2}$ in solution must be high in order to explain the zero-order dependence observed in Ref. [28]. The inhibitory effect of CO and SX is represented by the $K_4 P_{\text{CO}}$ and the $K_5 [\text{SX}]$ terms in the denominator, respectively. The order with respect to CO becomes less negative in presence of SX due to the term $K_5 [\text{SX}]$ also present in the denominator of Eq. (1).

The parameters appearing in Eq. (1) for Shvo/SiO₂ and SX-Shvo/SiO₂ were estimated using the data fitting routine (i.e. "nlinfit" function) in MATLAB with the initial guesses of the parameters set to zero. Values for the parameters are listed in Table 3 for n - and iso-butanol formation. As seen in Fig. 4a–d, the derived rate expression given in Eq. (1) describes the experimental data effectively. The coefficient of determination, R^2 , is above 90% for all cases considered. Values of R^2 , the root-mean-square error (RMSE), and a parity plot are presented in the Supporting information.

Table 3

Values of the rate parameters appearing in Eq. (1) obtained by a best fit to experimental data.

Parameter	Value	Unit
K_2	30	atm ⁻¹
K_4	55	atm ⁻¹
K_5	7.3×10^6	m ² atm ⁻¹
k_3	255 ^a	
	325 ^b	atm ⁻¹ h ⁻¹

^a n -Butanol.

^b iso-Butanol.

3.4. Butene hydrogenation over Shvo/SiO₂

The hydrogenation of 1-butene was investigated in order to determine activity of Shvo/SiO₂ for hydrogenation of alkenes. It was observed that the 1-butene hydrogenation activity was 0.4 h⁻¹, which is more than an order of magnitude lower than the activity for butanal hydrogenation under comparable conditions. Consistent with our results, Shvo and coworkers demonstrated that the alkenes are unreactive for hydrogenation in the presence of Shvo's Catalyst and formic acid [29]. The difference in hydrogenation activity between 1-butene and butanal is attributable to the non-polarity of 1-butene. Accordingly, 1-butene is unable to coordinate to the hydridic and acidic hydrogen atoms on the Ru cluster as effectively as the polar carbonyl of butanal.

3.5. Tandem hydroformylation and hydrogenation using Rh-SILP and Shvo/SiO₂ catalysts

The direct conversion of propene to butanol was investigated using a bi-layered catalyst bed of SX-Rh SILP and Shvo/SiO₂. The SX-Rh SILP catalyst was selected because of its high activity and stability for propene hydroformylation [13]. Our previous study of Rh-SILP catalysts showed that catalysts containing the SX ligand were almost six times more active than catalysts prepared with triphenylphosphine or sulfonated triphenyl phosphine ligands [13]. We have also demonstrated that at 363 K, the apparent partial pressure dependencies of propene, H₂, and CO are 0.93, 0.1, and -0.43 [14]. However, the apparent partial pressure dependencies of propene, H₂, and CO become 0.76, 0.84, and zero, respectively at 413 K. Since the kinetics of butanal hydrogenation exhibit a nearly first-order dependence on H₂ and an inverse dependence on the partial pressure of CO (see Table 2), a high ratio of H₂ to CO partial pressures is desired. The reaction temperature was set to 413 K to exploit first-order and zero-order dependence of H₂ and CO on the rates of propene hydroformylation and to lower the molar ratio of n -butanal to iso-butanol (n/i) formation. A low n/i ratio is desirable for fuel production because the anti-knock index of iso-butanol is much greater than n -butanol [4]. The CO and propene partial pressure were fixed at 0.25 atm, while the H₂ partial pressure was varied from 0.25 to 2.5 atm. As shown in Fig. 5, the propene conversion to butanal and the aldehyde conversion to butanol rises as the H₂/CO molar ratio is increased. Also shown in Fig. 5 is the predicted propene and aldehyde conversion as calculated from the rate laws presented in this work and in Ref. [14]. For convenience, the values of the parameters in the hydroformylation rate expression measured at 413 K are provided in Table 4. As expected from our previous work on hydroformylation and this work, the molar ratios of n -butanal to iso-butanal and n -butanol to iso-butanol were both approximately 7. Under the most favorable conditions examined (H₂/CO = 10), 15% propene conversion and 90% aldehyde conversion were observed; thus, a 13% yield to butanol was achieved. The results presented in Fig. 5 illustrate, to the best of our knowledge, the first example of the direct conversion of propene to butanol by means of the tandem hydroformylation and hydrogenation reactions carried out in the gas phase using heterogeneous catalysts.

The rate expressions of hydroformylation and hydrogenation were also used to predict the conditions necessary to achieve a high yield of butanol from propene over SX-Rh SILP and Shvo/SiO₂ catalysts. Fig. 6 shows the effects of varying the total pressure on the minimum amount of hydroformylation catalyst and hydrogenation catalyst necessary to achieve 99% conversion in each reaction. In all of the cases examined, the initial molar flow rate of the feed is set to 54 mmol h⁻¹ and the inlet feed consists of a 1:1:2 M ratio of C₃H₆:CO:H₂. Under these conditions, Shvo/SiO₂ operates in the absence of CO because 99% of the propene and

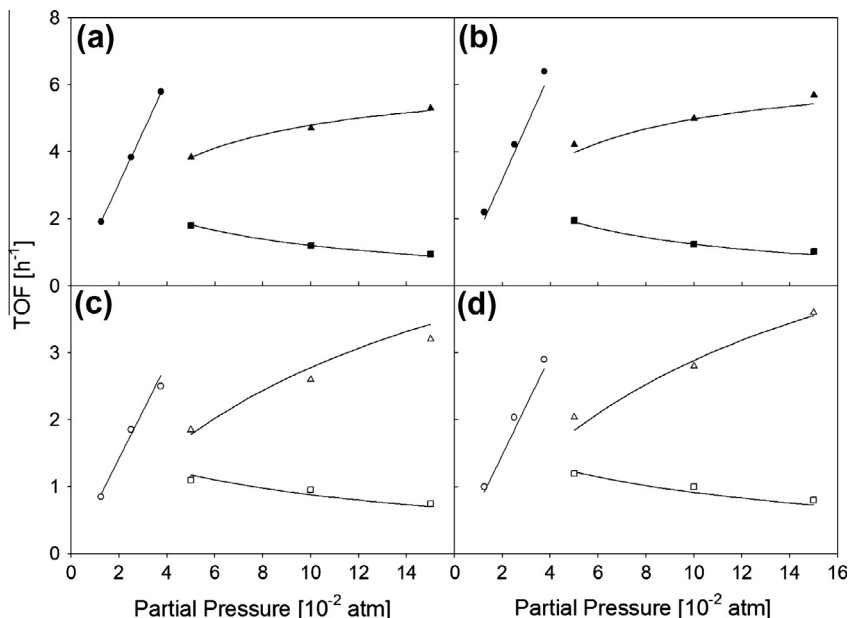


Fig. 4. (a–d) Non-linear regression of partial pressure data using (a,b) Shvo/SiO₂ and (c,d) SX-Shvo/SiO₂. Rate of (a,c) *n*- and (b,d) iso-butanol synthesis vs. partial pressure of (●,○) butanal, (▲,△) H₂, and (■,□) CO. Experimental points are indicated by data markers. Spline curves indicate predicted values. *T* = 363 K, *P*_{Total} = 1 atm, catalyst mass = 0.3 g, total gas flow rate = 100 cm³ min⁻¹.

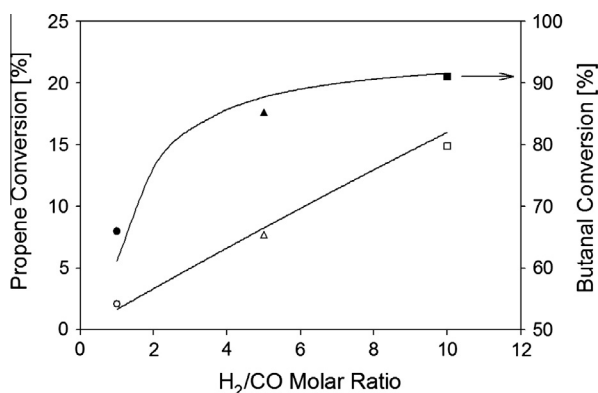


Fig. 5. Results from tandem hydroformylation–hydrogenation experiment. *T* = 413 K. (○,△,□) Propene conversion to butanol. (●,▲,■) Butanol conversion to butanol. *P*_{C₃H₆} = *P*_{CO} = 0.25 atm. (○,●) *P*_{H₂} = *P*_{H₂}⁰ = 0.25 atm, (△,▲) *P*_{H₂} = 1.25 atm, (□,■) *P*_{H₂} = 2.5 atm. SX-Rh SILP catalyst mass = 0.4 g (0.2 wt.% Rh), Shvo/SiO₂ = 0.8 g (1 wt.% Ru). The solid lines represent conversions determined from the rate expressions for propene hydroformylation and butanol hydrogenation (Eq. (1)).

Table 4

Rate parameters determined for propene hydroformylation over SX-Rh SILP Ref. [14].

$$r_{\text{butanol}} = \frac{aP_{\text{C}_3\text{H}_6}P_{\text{H}_2}[\text{Rh}]}{1+b(1+K_5)P_{\text{C}_3\text{H}_6}}$$

Parameter	Value		Unit
	<i>n</i> -Butanol	iso-Butanol	
$a = K_1K_2K_3K_4K_5k_6$	589	85.6	atm ⁻² h ⁻¹
$b = K_1K_2K_3K_4$	0.89	0.22	atm ⁻¹
K_5	0.20	1.8	–
$k_6 = a(bK_5)^{-1}$	3287	210	atm ⁻¹ h ⁻¹

CO are consumed in the hydroformylation reaction. Fig. 6 shows the amount of catalyst necessary to achieve a 98% yield of butanol decreases substantially as the total pressure is increased. While the span of experimental conditions predicted are beyond the limitations of the apparatus available for the present study, it is evident

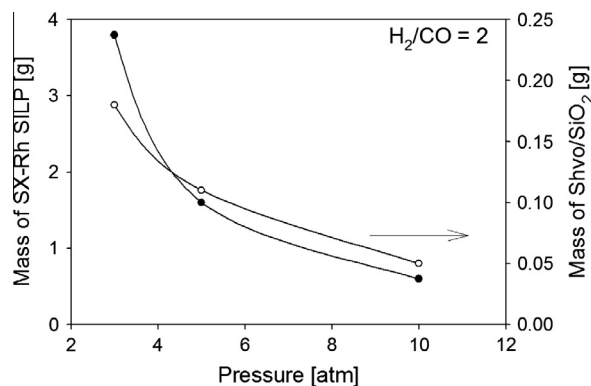


Fig. 6. Modeled results of the tandem hydroformylation–hydrogenation experiment. (●) Mass of SX-Rh SILP catalyst and (○) mass of Shvo/SiO₂ catalyst necessary to achieve 98% yield to butanol as a function of total pressure. *T* = 413 K, *N_T* = 54 mmol h⁻¹, 2*P*_{C₃H₆} = 2*P*_{CO} = *P*_{H₂}.

that a high yield of butanol could be achieved starting with a stoichiometric feed of propene and synthesis gas.

4. Conclusion

The kinetics of butanol hydrogenation over Shvo/SiO₂ and SX-Shvo/SiO₂ have been investigated. The activity of SX-Shvo/SiO₂ was lower than the activity of Shvo/SiO₂, but the apparent activation energies for hydrogenation of *n*- and iso-butanol were nearly identical (~50 kJ mol⁻¹) for both catalysts. This result suggests that the catalytically active species is the same for both catalysts. The partial pressure dependence on butanal is roughly first order for both catalysts, while the partial pressure dependence on H₂ is ~0.3 and 0.4 for Shvo/SiO₂ and SX-Shvo/SiO₂, respectively. Similarly, the partial pressure dependence on CO increases from –0.6 in the absence of SX to –0.3 in the presence of SX. The differences in the orders in the partial pressures of H₂ and CO are ascribed to the coordination of SX to Ru, which was confirmed by in situ

infrared spectroscopy and ^{31}P MAS NMR. Infrared spectroscopy also provided evidence for several of the intermediates appearing in the mechanism shown in Scheme 1. Based upon the proposed mechanism, the ability of Shvo's catalyst to function in the presence of CO is attributed to the competition between a vacant coordination site and the addition of a H_2 to the Ru complex. A rate law was derived assuming that the reduction of aldehyde is the rate-determining step (Reaction 3 in Scheme 1) and that the other elementary steps are quasi-equilibrated. The rate coefficients appearing in Eq. (1) were obtained by non-linear regression (see Table 3) and found to describe the experimental data very well.

The direct gas-phase conversion of propene to butanol was demonstrated for the first time using a bi-layered, packed-bed reactor containing SX-Rh SILP, and Shvo/ SiO_2 catalysts. Under the conditions investigated, the overall yield a 13% to *n*- and iso-butanol ($n/i = 7$) was achieved using a feed molar ratio of $\text{H}_2/\text{CO} = 10$. This proof-of-concept experiment demonstrates the feasibility of converting propene to butanol in a single reactor. The rate expressions describing the kinetics of propene hydroformylation and butanal hydrogenation were also used to predict the amount of each catalyst required to achieve a 98% yield of butanol as a function of total pressure for an assumed stoichiometric feed and initial molar flow rate.

Acknowledgment

This work was supported by the XC² program funded by BP.

Appendix A. Supplementary material

Supplementary data associated with this article can be found, in the online version, at <http://dx.doi.org/10.1016/j.jcat.2013.11.012>.

References

- [1] A. Chauvel, G. Lefebvre, in: *Petrochemical Processes*, second ed., Editions Technip, Paris, 1989, pp. 81–90.
- [2] P. Durre, *Ann. N. Y. Acad. Sci.* 1125 (2008) 353.
- [3] S. Lee, M.O. Cho, C.H. Park, Y. Chung, J.H. Kim, B. Sang, Y. Um, *Energy Fuels* 2 (2008) 3459.
- [4] E. Christensen, J. Yanowitz, M. Ratcliff, R.L. McCormick, *Energy Fuels* 25 (2011) 4723.
- [5] J.E. Rekoske, M.A. Barteau, *Ind. Eng. Chem. Res.* 50 (2011) 41.
- [6] S. Marengo, P. Comotti, G. Galli, *Catal. Today* 81 (2003) 205.
- [7] Y. Lee, J.H. Park, S.H. Jang, L.K. Nielsen, J. Kim, K.S. Jung, *Biotechnol. Bioeng.* 101 (2008) 209.
- [8] F. Coloma, A. Sepulveda-Escribano, J.L.G. Fierro, F. Rodriguez-Reinoso, *Appl. Catal., A* 136 (1996) 231.
- [9] P. Reyes, M.C. Aguirre, J.L.G. Fierro, G. Santori, O.J. Ferretti, *Mol. Catal. A: Chem.* 184 (2002) 431.
- [10] J.K. Jeon, J.H. Yim, Y.K. Park, *Chem. Eng. J.* 140 (2008) 555.
- [11] A. Riisager, K.M. Eriksen, P. Wasserscheid, R. Fehrmann, *Catal. Lett.* 90 (2003) 149.
- [12] A. Riisager, R. Fehrmann, M. Haumann, B.S.K. Gorle, P. Wasserscheid, *Ind. Eng. Chem. Res.* 44 (2005) 9853.
- [13] S. Shylesh, D.G. Hanna, S. Werner, A.T. Bell, *ACS Catal.* 4 (2012) 487.
- [14] D.G. Hanna, S. Shylesh, S. Werner, A.T. Bell, *J. Catal.* 292 (2012) 166.
- [15] D. Konya, K.Q. Almeida Lereno, E. Lereno, *Organometallics* 23 (2006) 3166.
- [16] J. Zakzeski, H.R. Lee, Y.L. Leung, A.T. Bell, *Appl. Catal., A* 374 (2010) 201.
- [17] K. Takahashi, M. Yamashita, T. Ichihara, K. Nakano, K. Nozaki, *Angew. Chem. Int. Ed.* 49 (2010) 4488.
- [18] W.P. Mul, K. Ramkisoensing, P.C.J. Kamer, J.N.H. Reek, A.J. van der Linden, A. Marson, P.W.N.M. van Leeuwen, *Adv. Synth. Catal.* 344 (2002) 293.
- [19] L.Q. Xu, V.L. Zholobenko, L.M. Kustov, W.M.H. Sachtler, *J. Mol. Catal.* 83 (1993) 391.
- [20] J.F. Joly, N. Zanier-Szydowski, S. Colin, F. Raatz, J. Saussey, J.C. Lavalley, *Catal. Today* 9 (1991) 31.
- [21] Y. Shvo, D. Czarkie, Y. Rahamim, *J. Am. Chem. Soc.* 108 (1986) 7400.
- [22] N. Menashe, Y. Shvo, *Organometallics* 10 (1991) 3885.
- [23] J.S.M. Samec, J.E. Backvall, P.G. Andersson, P. Brandt, *Chem. Soc. Rev.* 35 (2006) 237.
- [24] J.E. Caton, C.V. Banks, *Inorg. Chem.* 6 (1967) 1670.
- [25] M.J. Mays, M.J. Morris, P.R. Raithby, Y. Shvo, D. Czarkie, *Organometallics* 8 (1989) 1162.
- [26] C.P. Casey, S.E. Beetner, J.B. Johnson, *J. Am. Chem. Soc.* 130 (2008) 2285.
- [27] R.H. Crabtree, Carbonyls, phosphine complexes, and ligand substitution reactions, in: *The Organometallic Chemistry of the Transition Metals*, fourth ed. John Wiley & Sons, Inc., Hoboken, 2005, p. 101.
- [28] C.P. Casey, N.A. Strotman, S.E. Beetner, J.B. Johnson, D.C. Priebe, T.E. Vos, B. Khodavandi, I.A. Guzei, *Organometallics* 25 (2006) 1230.
- [29] N. Menashe, E. Salant, Y. Shvo, *J. Organomet. Chem.* 514 (1996) 97.